THE JOURNAL OF PHYSICAL CHEMISTRY A

Article

pubs.acs.org/JPCA

Crossed Molecular Beams Studies of Phenyl Radical Reactions with Propene and *trans*-2-Butene

Daniel R. Albert, Michael A. Todt, and H. Floyd Davis*

Department of Chemistry and Chemical Biology, Baker Laboratory, Cornell University, Ithaca, New York 14853-1301, United States

ABSTRACT: The reactions of phenyl radicals with propene have been studied at collision energies of 84 and 108 kJ/mol using the crossed molecular beams technique. The branching ratios between methyl radical elimination forming C_8H_8 and H-atom elimination forming C_9H_{10} were found to be 10 ± 1:1 at 84 kJ/mol and 3 ± 1:1 at 108 kJ/mol. By using "soft" 9.9 eV vacuum ultraviolet photoionization for product detection, we were able to observe both product channels with negligible fragmentation of C_9H_{10} to $C_8H_8^+$. Our finding that CH_3 elimination is dominant is consistent with conclusions from a recent study employing a pyrolysis molecular beam reactor using photoionization detection. However, our C_8H_8/C_9H_{10} branching ratios are significantly larger than inferred from previous CMB experiments and RRKM calculations. For comparison, we have also studied the reactions of phenyl radicals with *trans*-2-butene at E_{coll} = 97 kJ/mol. In this case, the symmetry of *trans*-2-butene makes both alkene addition sites chemically equivalent. The intermediate formed in the reaction with *trans*-2-butene is similar to the 2-carbon addition intermediate in the reaction with propene. We observed only methyl elimination in the reaction with *trans*-2-butene, with no evidence for H-atom elimination, consistent with conclusions that C−C bond fission is the most favorable channel in these systems. Analogies between phenyl radical reactions with propene and *trans*-2-butene are used to provide insight into the mechanisms in the propene reaction.

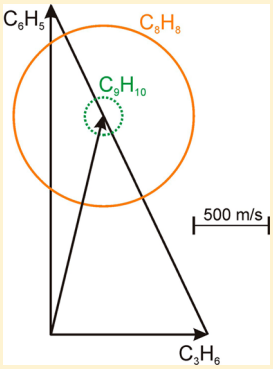

INTRODUCTION

The reactions of phenyl radicals (C_6H_5) in combustion environments have long been established as benchmarks for understanding the role of cyclic aromatic species, particularly in the formation of soot.[1,2] Soot formation is initiated by the formation of polycyclic aromatic hydrocarbons (PAHs), which can then aggregate to form the nano/micro sized particles that cause a wide variety of environmental and health issues.[3,4] The reaction of phenyl radicals with unsaturated hydrocarbons is thought to be one of the key initiation processes in the synthesis of PAHs. The electron deficient phenyl radical site can add to the π-electronic system of an unsaturated hydrocarbon, forming a branched aromatic species that can then continue to grow via the HACA (hydrogen abstraction, acetylene addition) mechanism or other hydrocarbon addition mechanisms.[5,6]

Considerable work was carried out by Lin and co-workers aimed at understanding this class of reactions.[7−9] In order to accurately test the prediction of product branching ratios using calculated potential energy surfaces, the identification and quantification of primary product channels as a function of available energy is necessary. Crossed molecular beam (CMB) reactive scattering experiments serve as a valuable technique for elucidating product branching ratios and reaction mechanisms under single collision conditions.[10−12]

In the reaction of C_2 hydrocarbons with phenyl radicals, the only predicted primary products involve H-atom abstraction from the C_2 hydrocarbon, $C_6H_5 + C_2H_x \rightarrow C_6H_6 + C_2H_{x-1}$, or addition to an unsaturated hydrocarbon followed by H-atom elimination, $C_6H_5 + C_2H_x \rightarrow C_6H_5C_2H_{x-1} + H$.[7,8] When phenyl radicals react with larger unsaturated hydrocarbons, the same H-atom abstraction and elimination pathways exist in addition to other elimination products (CH_3, C_2H_5, etc.) that form larger aromatic species.[9]

The reaction of phenyl radicals with propene was studied as early as 1972, when Hefter and co-workers examined the addition products by electron spin resonance at 183 K in liquid propene.[13] They found evidence of three pathways: addition to the 1-carbon, addition to the 2-carbon, and H-atom abstraction forming benzene plus allyl radicals.

Park et al. studied the consumption of phenyl radicals in the presence of propene using cavity ring-down spectroscopy, finding the rate constant at low temperatures (296−496 K) to be $\sim 10^{12}$ cm^3 mol^{-1} s^{-1}.[9] In addition they calculated stationary points along the reaction coordinates for many of the key reaction pathways. On the basis of calculated potential energy barriers, Park et al. predicted that addition to the 1-carbon atom in propene is the dominant addition channel over their temperature range. The addition to the 2-carbon atom was predicted to involve a barrier 5−10 kJ mol^{-1} higher than the addition to the 1-carbon atom.[9]

The first CMB experiments were conducted at collision energies between 130 and 194 kJ mol^{-1}.[14,15] Under these conditions, only the H-atom elimination channel was observed, with an upper limit of 10% placed on the possible methyl elimination channel producing styrene (C_8H_8).[15] From experiments employing deuterium-substituted propene, it was concluded that ∼85% of the H-atoms were emitted from the

Received: August 9, 2013
Revised: November 21, 2013
Published: November 25, 2013

1- and 2-carbon atoms, with the other ∼15% coming from the methyl group.[14,15] This result was consistent with expectations that H-atoms bound to the 1- and 2-carbon atoms in the addition intermediate are more weakly bound than those in the methyl group.[9]

In a reinvestigation of the reaction of phenyl radicals with propene at a much lower collision energy (45 kJ/mol), methyl-elimination forming C_8H_8 was observed, along with the previously identified H-atom elimination pathways.[16] The product branching ratio between the methyl and H-atom elimination was found to be ∼2:1, in apparent agreement with RRKM calculations that accompanied the experimental work.[16] The RRKM calculations predicted that methyl radical elimination forming styrene (C_8H_8) (calculated to be exoergic by 70 kJ/mol) should be dominant at low collision energies, with H-atom elimination forming C_9H_{10} becoming dominant at collision energies above 100 kJ/mol. Possible isomers of C_9H_{10} and their calculated energetics relative to the reactants are 2-phenylpropene (−31 kJ/mol), *cis*- and *trans*-1-phenylpropene (−24 and −32 kJ/mol) and 3-phenylpropene (−13 kJ/mol).[16] In contrast to the earlier CMB study[15] where 3-phenylpropene was found to be the minor H-atom elimination channel, this isomer was predicted by RRKM calculations to be the dominant C_9H_{10} product.[16] The preferential fission of the more strongly bound H-atoms from the methyl group (fission at the 3-carbon) was attributable to the potential energy barrier being about 1 kJ/mol smaller than for C−H fission at the 1- or 2-carbon atoms.[16]

In more recent work carried out at Berkeley's Advanced Light Source, the reactions of phenyl radicals with propene were studied using a pyrolysis molecular beam reactor.[17] Nitrosobenzene, which undergoes pyrolysis to form phenyl radicals and nitrogen monoxide, was coexpanded with propene carrier gas in a high temperature pyrolysis nozzle source where the phenyl radicals can subsequently react with propene. Products were probed using soft tunable vacuum ultraviolet (VUV) single photon ionization using a synchrotron. The authors were able to identify the methyl elimination channel forming C_8H_8, as well as H-atom elimination forming, C_9H_{10}. At the estimated temperature of the pyrolysis tube (1200−1500 K), formation of C_8H_8 was found to be dominant with a branching ratio of 6:1 for C_8H_8/C_9H_{10}.[17] The contribution from $C_8H_8 + CH_3$ relative to $C_9H_{10} + H$ inferred from the photoionization study is thus much larger than from the CMB study[16] or from the RRKM calculations.[16,18]

Product photoionization efficiency curves can, under favorable conditions, be used to distinguish between chemical isomers having different ionization energies (I.E.).[19,20] In the reaction of phenyl + propene, the C_8H_8 product produced in the pyrolysis molecular beam reactor was identified as styrene, the lowest energy C_8H_8 isomer.[17] The photoionization efficiency curves for the C_9H_{10} products were found to be consistent with primary formation of the 3-phenylpropene isomer, with a very small yield of the *cis*- and *trans*-1-phenylpropene (i.e., opposite to the previous CMB results[16]), with no evidence for production of the cyclic indane isomer.[17]

Here, we report studies of reactions of phenyl radicals with propene at collision energies of 84 and 108 kJ/mol using 9.9 eV single photon ionization of reaction products. To gain further insight into the $C_6H_5 + C_3H_6$ reaction, we also have performed CMB studies of the reaction of phenyl radical with *trans*-2-butene (C_4H_8).

EXPERIMENTAL SECTION

The experiments were performed using the Cornell rotatable source, fixed detector crossed molecular beams apparatus, which has been described in detail previously.[21] The phenyl radical beam (velocity = 2250 m/s; speed ratio = 13) was produced by bubbling H_2 carrier gas (∼1800 Torr) through room-temperature, liquid chlorobenzene (Sigma-Aldrich) (∼10 Torr), expanding the gas mixture through the 1 mm orifice of a piezoelectrically actuated pulsed valve[22,23] and photolyzing (6 mm × 2 mm spot size) chlorobenzene with the laser beam axis orthogonal to the molecular beam axis and aligned immediately in front orifice of the pulsed valve orifice. The 193 nm photolysis of chlorobenzene produced primarily phenyl radicals and chlorine atoms.[12,24,25] The 193 nm photons (∼10 mJ per pulse) were generated with an ArF excimer laser (GAM EX10) that was attached to the rotating source flange in order to maintain constant alignment at all source angles. The phenyl radical beam passed through a 2 mm skimmer before entering the scattering chamber. Molecular beams of propene (Aldrich) and *trans*-2-butene (Aldrich) were generated by expanding a mixture of C_3H_6 or C_4H_8 in H_2 or He carrier gas through a second 1 mm piezoelectric pulsed valve. Beam velocities, speed ratios, and collision energies for the C_3H_6 and C_4H_8 molecular beams are summarized in Table 1. The molecular beam passed through a 2 mm diameter skimmer before intersecting the phenyl radical beam at a 90° crossing angle.

Table 1. Beam Parameters for Studied Phenyl Radical Reactions

gas mixture	beam velocity (m/s)	speed ratio ($v/\Delta v$)	collision energy (kJ/mol)	CM angle (degrees)
25% C_3H_6 in He	1050	12	84	14
9% C_3H_6 in H_2	1700	10	108	22
25% C_4H_8 in He	960	12	97	17

The molecular beams were characterized in a separate series of experiments by chopping the beam with a slotted chopper wheel and measuring the on-axis time-of-flight (TOF) distributions using electron impact ionization detection.[12] The phenyl radical beam and reactive scattering TOF distributions were measured using VUV photoionization detection.[12] Scattered species traveled ∼25 cm to a triply differentially pumped detector region (∼10^{-10} Torr) where they were ionized using either the electron impact ionization detector or the VUV photoionization detector.[26] The positive ions were then mass selected using a quadrupole mass filter (Extrel) and detected using a conversion dynode/electron multiplier in pulse counting mode.

The pulsed VUV light at 9.9 eV was generated by resonance enhanced four-wave mixing in Hg vapor through the two-photon resonance at 63 928 cm^{-1} using unfocused commercial lasers.[26−28] The fourth harmonic (266 nm) of an injection seeded Nd:YAG laser (Continuum 9030) along with 380 nm light summed to the two photon resonance (63 928 cm^{-1}), and a third photon (∼630 nm) was tuned to phase match near the 9P resonance in Hg. The 380 nm radiation was generated by mixing the 580 nm output of a 532 nm pumped dye laser (Scanmate 2, Kiton Red dye) with the fundamental (1064 nm) of the seeded Nd:YAG laser. The 630 nm radiation was

dx.doi.org/10.1021/jp407986n | J. Phys. Chem. A 2013, 117, 13967−13975

produced directly from a 532 nm pumped dye laser (Scanmate 2, DCM dye). All three lasers were aligned spatially and temporally through a 1 m long Hg heat pipe (~400 K). A slow flow of ~10 Torr of He buffer gas was maintained from the ends of the cell toward the center to keep the optics clean. The VUV was spatially dispersed from the ultraviolet and visible beams by off-axis transmission through a 50 cm focal length MgF_2 lens (ISP Optics). The ultraviolet and visible beams were physically blocked from entering the detector by a ceramic beam dump mounted to a translation stage, while the VUV passed by the beam dump and entered the ionization region of the triply differentially pumped detector.

The TOF distributions were generated by stepping the VUV laser relative to the 193 nm photolysis laser. The product flux distribution was measured by rotating the source assembly relative to the detector and measuring TOF arrival distributions at each angle. Laboratory angular distributions were generated by integrating the TOF arrival distributions at each angle. The experimental data was fitted using the forward convolution technique described previously.[29] A computer program took as inputs a center of mass translational energy distribution, $P(E)$, a center of mass angular distribution, $T(\Theta)$, and known instrument and beam parameters and outputted simulated TOF spectra and laboratory angular distributions. The two center of mass functions, $P(E)$ and $T(\Theta)$, were then iteratively adjusted until agreement was reached between the measured and simulated TOF spectra and laboratory angular distributions.

RESULTS AND DISCUSSION

C_6H_5 + C_3H_6 Experiments. The TOF distributions for C_6H_5 + C_3H_6 at E_{coll} = 84 kJ/mol, monitoring the formation of C_9H_{10} + H and C_8H_8 + CH_3, are shown in Figures 1 and 2, respectively. The H-atom elimination products were monitored at m/e = 118 ($C_9H_{10}^+$) and methyl elimination products were monitored at m/e = 104 ($C_8H_8^+$). The corresponding laboratory angular distributions are shown in Figure 3. The best fit CM functions for both channels are shown in Figure 4. The best fit $T(\Theta)$ is forward−backward symmetric for both product channels, consistent with the participation of collision complexes with lifetimes greater than their picosecond rotational time scales. The isotropic angular distribution, i.e., a flat $T(\Theta)$, is a consequence of angular momentum conservation and the geometric structure of the intermediate complex, as discussed in detail elsewhere.[29] The best fit $P(E)$ for the methyl elimination product channel peaks at ~35 kJ/mol, with a mean kinetic energy release of 48 kJ/mol. Thus, at this collision energy, 31% of the total available energy (154 kJ/mol) appears in product translational energy. For a 20 atom polyatomic system such as this, the appearance of a relatively large fraction of available energy in product translational energy suggests the existence of an exit barrier for the formation of C_8H_8 + CH_3, consistent with theoretical predictions.[9,16,18] The best fit $P(E)$ for the H-atom elimination products is broad, with an average of 50 kJ/mol appearing in product translation. This corresponds to 43% of the available energy (115 kJ/mol), which again is a relatively large fraction for a polyatomic system of this complexity. We note that due to the kinematics of detecting a heavy species recoiling from an H-atom, the uncertainty in the $P(E)$ is much larger than that for the methyl elimination channel.

The Newton diagrams for each product channel (Figure 5) illustrate the difference in the kinematics of the two product

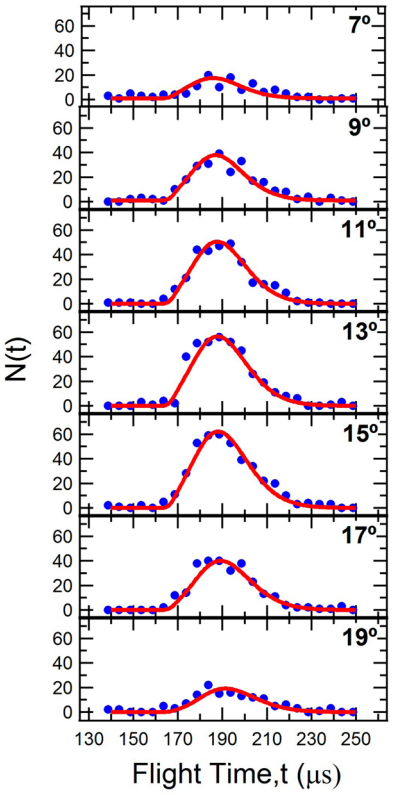

Figure 1. TOF spectra monitoring $C_9H_{10}^+$ (m/e = 118) from the C_6H_5 + C_3H_6 → C_9H_{10} + H reaction, E_{coll} = 84 kJ/mol. Solid dots represent experimental data points; solid lines are calculated using the optimized CM distribution functions shown in Figure 4.

channels. The small Newton circle for H-atom elimination constrains the C_9H_{10} products to angles and velocities near that of the center of mass velocity vector. Consequently, the widths of the TOF and lab angular distributions are largely determined by the width of the center of mass velocity vector, especially in the case when the $P(E)$ peaks near zero translational energy release. At a given angle, a larger fraction of the total H-atom elimination products are observed relative to those for methyl-elimination products (Figure 5). The product branching ratio at E_{coll} = 84 kJ/mol was found to be 10 ± 1:1 for C_8H_8/C_9H_{10}.

The determination of product branching ratios must take into account the relative detection sensitivities for both products. In order to quantify the detection sensitivity for C_8H_8 and C_9H_{10}, we have monitored nonreactive scattering of molecular beams of styrene (Aldrich, C_8H_8) and alpha-methyl styrene (Aldrich, C_9H_{10}) using both a 100 eV electron impact ionization and 9.9 eV photoionization. By comparing the signal levels using both detection schemes, we found that the 9.9 eV photoionization cross-section for both species are equal to within our experimental uncertainty. This is not surprising as similar molecules belonging to a particular class (alkane, alkene, monoaromatic species, etc.) often have comparable photoionization cross-sections at comparable energies above their ionization thresholds.[30,31] We anticipate that the other possible C_9H_{10} isomers, all of which have ionization energies within 0.2 eV,[17] have 9.9 eV photoionization cross-sections similar to alpha-methyl styrene.[17,32]

The dependence of internal energy on photoionization cross-section is relevant to the determination of product branching ratios.[33−35] The total available product energy is the sum of the

dx.doi.org/10.1021/jp407986n | J. Phys. Chem. A 2013, 117, 13967−13975

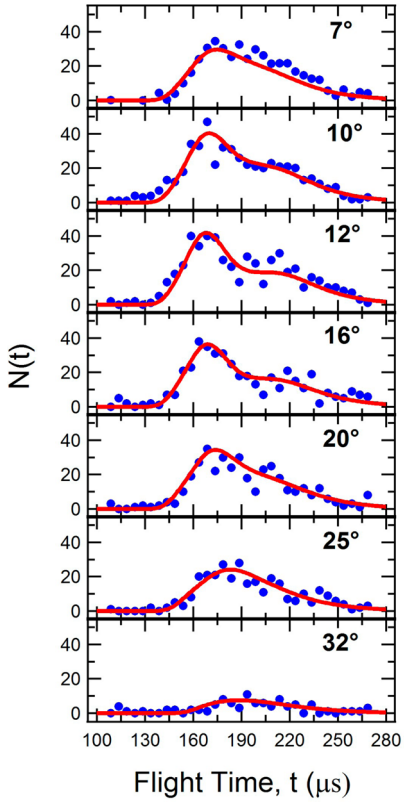

Figure 2. TOF spectra monitoring $C_8H_8^+$ (m/e = 104) from the C_6H_5 + C_3H_6 → C_8H_8 + CH_3 reaction, E_{coll} = 84 kJ/mol. Solid dots represent experimental data points; solid lines are calculated using the optimized CM distribution functions shown in Figure 4.

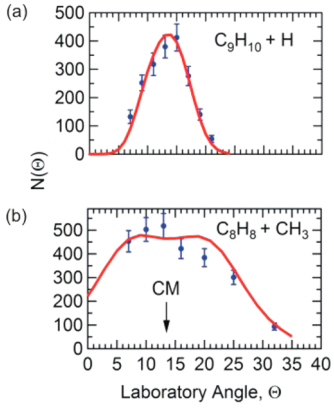

Figure 3. Laboratory angular distributions for the C_6H_5 + C_3H_6 reaction, E_{coll} = 84 kJ/mol. Solid dots represent experimental data points with 1σ error bars. Solid lines are calculated using the optimized CM distribution functions shown in Figure 4. (a) $C_9H_{10}^+$ (m/e = 118) from the C_6H_5 + C_3H_6 → C_9H_{10} + H reaction. (b) $C_8H_8^+$ (m/e = 104) from the C_6H_5 + C_3H_6 → C_8H_8 + CH_3 reaction.

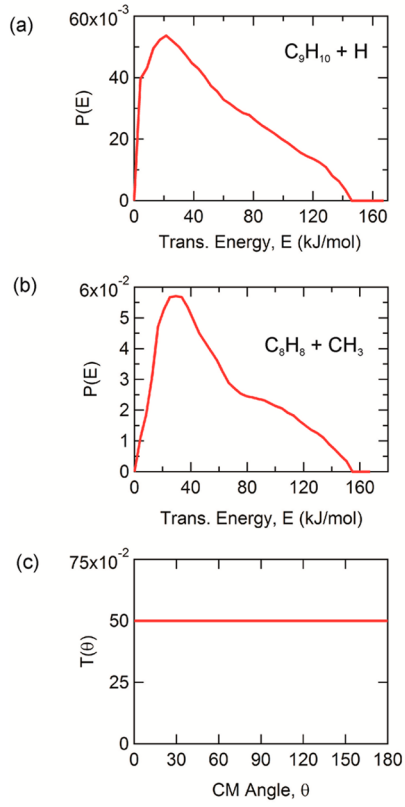

Figure 4. Optimized CM distributions for the C_6H_5 + C_3H_6 reaction, E_{coll} = 84 kJ/mol. (a) $P(E)$ for the C_9H_{10} products; (b) $P(E)$ for the C_8H_8 products; and (c) $T(\Theta)$ used for both C_9H_{10} and C_8H_8 products.

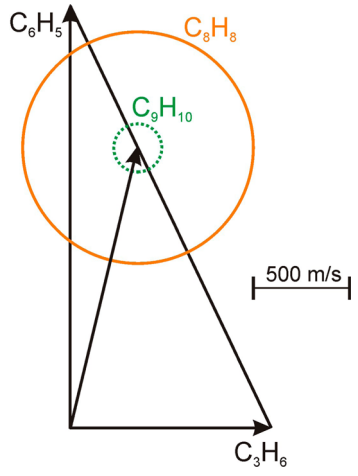

Figure 5. Newton diagram for the C_6H_5 + C_3H_6 reaction, E_{coll} = 84 kJ/mol. Dotted circle corresponds to the maximum C_9H_{10} velocities from C_6H_5 + C_3H_6 → C_9H_{10} + H. Solid circle corresponds to the maximum C_8H_8 velocities from C_6H_5 + C_3H_6 → C_8H_8 + CH_3.

collision energy, internal energy of reactants, and reaction exoergicity. This energy is distributed among internal degrees of freedom (vibration, rotation, etc.) of the product species and relative translational energy. In the data fitting procedure, the translational energy distribution, $P(E)$, is inferred; the total product internal energy distribution is found by subtracting the $P(E)$ from the total energy available. In the C_6H_5 + C_3H_6 reaction studied here, the total internal energy distribution is not much different for the C_8H_8 and C_9H_{10} reaction channels, ranging from 0 to 300 kJ/mol. The C_8H_8 product has a $P(E)$ that peaks further from zero than the C_9H_{10} product and will thus have a slightly lower internal energy contribution. The largest effect of internal energy on photoionization cross-section is seen near the photoionization threshold.[33−35] One obvious case of internal energy affecting the photoionization cross-section occurs with the ionization of product molecules below their 0 K ionization energy.[33,34] In this case, vibrationally

dx.doi.org/10.1021/jp407986n | J. Phys. Chem. A 2013, 117, 13967−13975

excited neutrals now have sufficient energy to reach the ground state of the ion, where their vibrationally unexcited counterparts do not. Also, when just above threshold, Franck−Condon factors can significantly affect the ionization efficiency if the ion has different equilibrium bond lengths than the neutral.[35] Recent studies probing this behavior have found that when molecules are ionized using single photon ionization that is well above the ionization threshold (>1 eV), the ionization efficiency is relatively independent of internal energy.[35−37] In the detection of C_8H_8 and C_9H_{10} at 9.9 eV, photoionization is carried out ∼1.5 eV above the ionization threshold,[17] and we do not expect the photoionization efficiency to be significantly altered by the internal energy of the products.

Both channels were also observed from the C_6H_5 + C_3H_6 reaction at E_{coll} = 108 kJ/mol. Time-of-flight arrival distributions for C_9H_{10} + H and C_8H_8 + CH_3 are shown in Figures 6 and 7, respectively. The lab angular distributions for

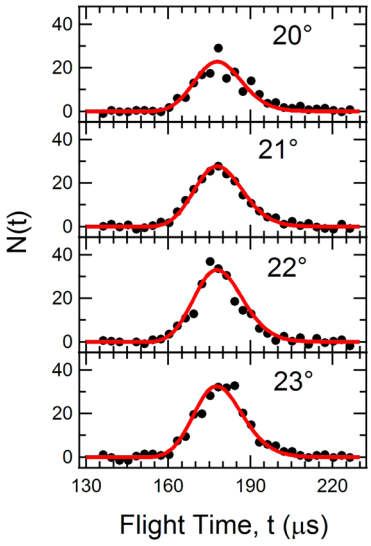

Figure 6. TOF spectra monitoring $C_9H_{10}^+$ (m/e = 118) in the C_6H_5 + C_3H_6 → C_9H_{10} + H reaction, E_{coll} = 108 kJ/mol. Solid dots represent experimental data points; solid lines are calculated using the optimized CM distribution functions shown in Figure 9.

both product channels are shown in Figure 8. The best fit center-of-mass angular distributions are again isotropic for both channels. The $P(E)$ for the C_8H_8 + CH_3 channel again peaks away from zero translational energy release (Figure 9). At this collision energy, 28% of the total available energy (178 kJ/mol) appears in product translational energy, which is similar to the value (31%) observed at the lower collision energy. Unfortunately, because of the kinematics of the H-atom channel, there is substantial uncertainty in the $P(E)$, particularly in the region of low translational energy at the higher collision energy. We used the same $P(E)$ for the H-atom channel at E_{coll} = 108 kJ/mol as was derived from the 84 kJ/mol data. The product branching ratio at E_{coll} = 108 kJ/mol is 3 ± 1:1 for C_8H_8/C_9H_{10}. Even at the increased collision energy of 108 kJ/mol, we thus measure a substantially larger contribution for the C_8H_8 channel than was predicted by RRKM calculations and measured in a previous crossed molecular beam scattering experiment by Kaiser et al.[16] at E_{coll} = 45 kJ/mol where a 2:1 branching ratio was measured. While we have not studied the reaction at collision energies below 84 kJ/mol, from the observed trend observed in our study we would anticipate

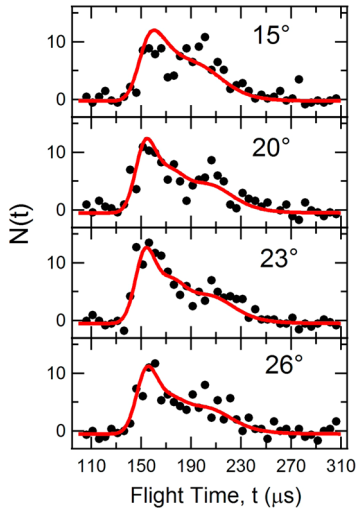

Figure 7. TOF spectra monitoring $C_8H_8^+$ (m/e = 104) in the C_6H_5 + C_3H_6 → C_8H_8 + CH_3 reaction, E_{coll} = 108 kJ/mol. Solid dots represent experimental data points; solid lines are calculated using the optimized CM distribution functions shown in Figure 9.

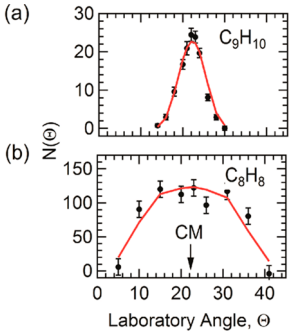

Figure 8. Laboratory angular distributions for the C_6H_5 + C_3H_6 reaction, E_{coll} = 108 kJ/mol. Solid dots represent experimental data points with 1σ error bars. Solid lines are calculated using the optimized CM distribution functions shown in Figure 9. (a) $C_9H_{10}^+$ (m/e = 118) from the C_6H_5 + C_3H_6 → C_9H_{10} + H reaction. (b) $C_8H_8^+$ (m/e = 104) from the C_6H_5 + C_3H_6 → C_8H_8 + CH_3 reaction.

branching ratios greater than 10:1. One complication in detecting the C_8H_8 product channel in the previous study using 80 eV electron impact was background from fragmentation of C_9H_{10} products to the parent mass of $C_8H_8^+$.[16] We are able to eliminate the fragmentation problem by using soft photoionization at 9.9 eV. Since the ionization energies of C_8H_8 and C_9H_{10} are both near 8.5 eV,[17,32] the use of photon energy close to the ionization threshold of the detected species minimizes dissociative ionization, allowing products to be detected exclusively at their parent mass.

In the C_6H_5 + C_3H_6 reaction, the phenyl radical can add to either the 1- or 2-carbon atom in propene, as illustrated in Figure 10a,b, respectively. On the basis of the calculations of Park et al.[9] and Kaiser et al.,[16] the addition to the 1-carbon proceeds over a slightly smaller barrier than the addition to the 2-carbon (∼5 kJ/mol for the addition to the 1-carbon and ∼10 kJ/mol for 2-carbon addition). In previous papers, considerable significance was attached to the relative barrier heights for addition, and mechanisms all focused on the 1-addition process as being dominant.[9,15,16] However, in the crossed molecular beams experiments to date, the collision energies are far above both the 1- and 2-addition barriers. Furthermore, it is well-

dx.doi.org/10.1021/jp407986n | J. Phys. Chem. A 2013, 117, 13967−13975

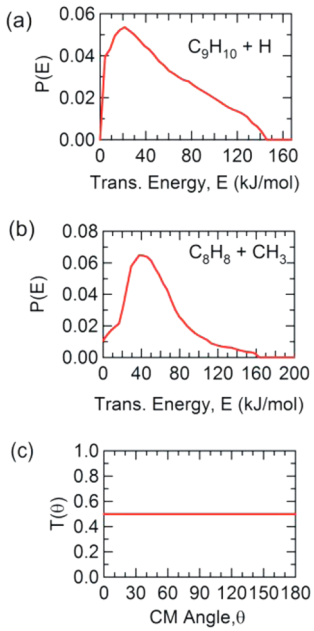

Figure 9. Optimized CM distributions for the C_6H_5 + C_3H_6 reaction, E_{coll} = 108 kJ/mol. (a) $P(E)$ for the C_9H_{10} products; (b) $P(E)$ for the C_8H_8 products; and (c) $T(\Theta)$ used for both C_9H_{10} and C_8H_8 products.

established that a low energy isomerization pathway allows rapid conversion between the 1-carbon vs 2-carbon addition intermediates.[9,16] This was confirmed in a recent RRKM study, which found that the rate constant for isomerization is substantially faster than decomposition.[16] Under these conditions, the relative importance of the addition to the 1-carbon or 2-carbon should not play a major role in determining the branching ratios between products. This conclusion is supported by comparisons of RRKM branching ratios assuming exclusive addition to the 1-carbon or 2-carbon atoms, which found that the branching ratios are nearly identical in both cases.[16] At very high collision energies (e.g., 200 kJ/mol) the product branching ratio for CH_3 elimination to H-atom elimination changes from 1:3.5 for exclusive addition to the 1-carbon to 1:2 for exclusive addition to the 2-carbon.[16] On the basis of these results, under our experimental conditions the initial phenyl radical addition site (1-carbon or 2-carbon) should have minimal influence on the final product branching ratios due to rapid isomerization. However, in discussing the reaction mechanisms, and in making comparisons with reactions involving *trans*-2-butene, it is important to remember that the 1-carbon and 2-carbon addition intermediates decay by different reaction pathways, with the 1-carbon intermediate decaying by R1 and R2, and the 2-carbon intermediate decaying by R3 and R4, as summarized in Figure 10.

As shown in Figure 10a, the most likely products from the 1-carbon addition intermediate involves formation of C_9H_{10} isomers (1-phenylpropene (R1) or 3-phenylpropene (R2)) by H-atom loss. From the 2-carbon addition intermediate (Figure 10b), because of the much weaker C−C bond relative to C−H, the likely decomposition product is C_8H_8 + CH_3 (R4), with H-atom loss producing 2-phenylpropene (R3) also possible. While we find the C_8H_8/C_9H_{10} branching ratio to be larger than in the previous crossed beams study and the accompanying RRKM calculations,[16] we observed a decrease from 10:1 at E_{coll} = 84 kJ/mol to 3:1 at E_{coll} = 108 kJ/mol,

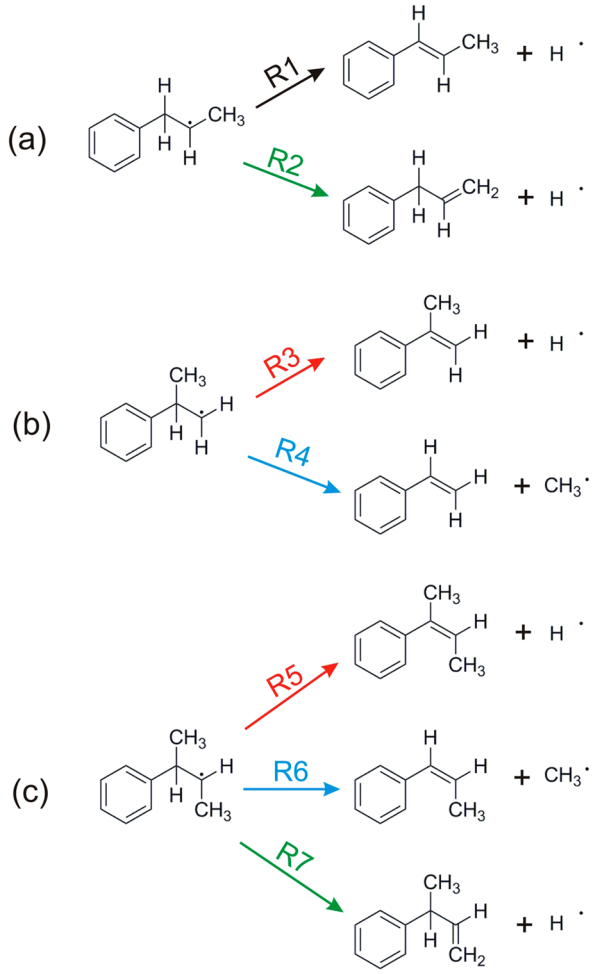

Figure 10. Schematic representation of addition intermediates and final product channels. (a) 1-Carbon addition intermediate in the C_6H_5 + C_3H_6 reaction. (b) 2-Carbon addition intermediate in the C_6H_5 + C_3H_6 reaction. (c) Addition intermediate in the C_6H_5 + C_4H_8 reaction. Analogous reactions between propene and *trans*-2-butene are R2/R7, R3/R5, and R4/R6.

consistent with the trend observed in the previous RRKM calculations.[16]

C_6H_5 + C_4H_8 Experiments. In an effort to gain additional insight into the propene reaction, we have also studied the phenyl radical reaction with *trans*-2-butene (C_4H_8). For this reactant, the 2- and 3-carbon atoms are *chemically equivalent*, and addition at both sites produces a common reaction intermediate, as illustrated in Figure 10c. This intermediate resembles that of the 2-carbon addition intermediate in the C_6H_5 + C_3H_6 reaction, (Figure 10b), due to the presence of both an H and CH_3 at the carbon atom addition site.

The C_9H_{10} TOF arrival time distributions at E_{coll} = 97 kJ/mol for the reaction C_6H_5 + C_4H_8 → C_9H_{10} + CH_3, are shown in Figure 11. The resulting laboratory angular and CM distributions are shown in Figures 12 and 13, respectively. The $P(E)$ peaks away from zero near 50 kJ/mol, implying that an exit barrier exists for the methyl elimination pathway. This is consistent with the behavior observed for the methyl-elimination channel in the C_6H_5 + C_3H_6 reaction. The $T(\Theta)$ is isotropic, suggesting the participation of collision complexes with lifetimes exceeding their rotational periods, as was observed in the propene reaction.

dx.doi.org/10.1021/jp407986n | J. Phys. Chem. A 2013, 117, 13967−13975

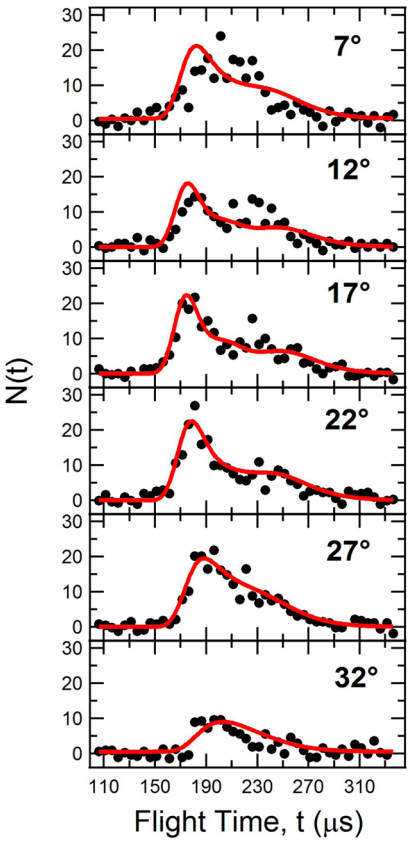

Figure 11. TOF spectra monitoring $C_9H_{10}^+$ (m/e = 118) in the C_6H_5 + C_4H_8 → C_9H_{10} + CH_3 reaction, E_{coll} = 97 kJ/mol. Solid dots represent experimental data points; solid lines are calculated using the optimized $P(E)$ shown in Figure 13 and an isotropic Θ identical to that shown in Figures 4 and 9.

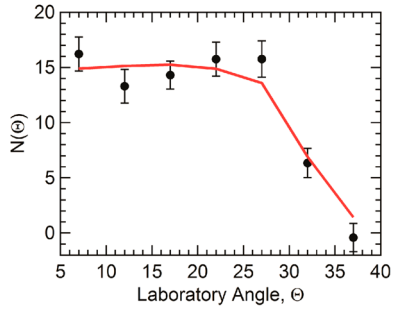

Figure 12. Laboratory angular distributions monitoring $C_9H_{10}^+$ from the C_6H_5 + C_4H_8 → C_9H_{10} + CH_3 reaction, E_{coll} = 97 kJ/mol. Solid dots represent experimental data points with 1σ error bars. Solid lines are calculated using the optimized $P(E)$ shown in Figure 13 and an isotropic Θ identical to that shown in Figures 4 and 9.

We carefully searched for the reaction C_6H_5 + C_4H_8 → $C_{10}H_{12}$ + H but found no evidence for its existence. Because of the kinematics of the reactions, our detection sensitivity for the H-atom elimination channel should be more than an order of magnitude larger than for methyl elimination. The photoionization cross-sections for phenyl products are similar, so no significant difference in detection sensitivity from differing photoionization cross-sections should exist.[30,31] From these considerations, we conclude that the H-atom elimination channel from C_6H_5 + C_4H_8 cannot account for more than

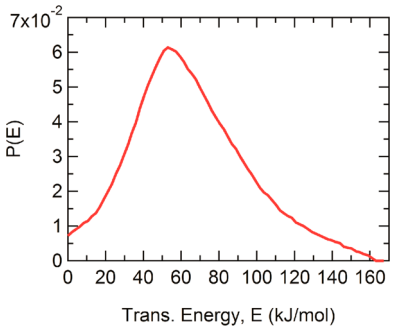

Figure 13. Optimized $P(E)$ distribution for the C_6H_5 + C_4H_8 → C_9H_{10} + CH_3 reaction, E_{coll} = 97 kJ/mol.

3% of the total reaction cross section. The dominance of C−C bond fission relative to C−H bond fission in these systems is a direct consequence of the much smaller C−C bond energy relative to C−H, as well as the smaller potential energy barrier for C−C bond fission relative to C−H fission. We now examine the reasons underlying the fact that C−H bond fission is observed in the propene reaction but not in the *trans*-2-butene system.

Propene Reaction Mechanism. The absence of the H-atom elimination channel in the *trans*-2-butene reaction is useful in understanding the propene reaction. The channels originating from the 2-carbon addition intermediate in the C_6H_5 + C_3H_6 reaction (Figure 10b) have analogues in the C_6H_5 + C_4H_8 reaction (Figure 10c): R3 is analogous to R5 because both involve H-atom elimination from the carbon atom adjacent to the phenyl group. Similarly, R4 is analogous to R6 because both involve CH_3 elimination from the carbon atom adjacent to the phenyl group. The C_6H_5 + C_4H_8 reaction intermediate can also lose a hydrogen atom from the methyl group (R7 in Figure 10) in a manner analogous to the C_6H_5 + C_3H_6 reaction (R2 in Figure 10) forming 3-phenylpropene. Reaction R1 in the propene system, involving H-atom elimination from a CH_2 moiety adjacent to the phenyl group, has no analogue in the butene system.

In the comparison of the butene and propene reactions, one must keep in mind that the cis steric repulsions in the alkene products differ slightly between the propene and butene systems, with the *cis*-methyl−methyl and methyl−phenyl repulsive interactions being slightly more important in the butene reactions. From these considerations, the H-atom elimination channels in the butene reactions are slightly less thermodynamically favorable (by a few kJ/mol) than are the analogous products in the propene system.

As noted above, the absence of H-atom products from the *trans*-2-butene reaction shows that the H-atom elimination reactions R5 and R7 cannot compete with the methyl elimination channel R6. Because of the above-noted similarity between intermediates in Figure 10b,c, H-atom elimination from the 2-carbon addition intermediate (R3) is not likely to be competitive with CH_3 elimination (R4). Despite the slightly different (at most a few kJ/mol) energetics between the propene and butene reactions due to the cis-steric interactions, the butene results provide strong evidence that H-atom elimination in the propene reaction primarily results from decomposition of the 1-addition intermediate, as illustrated in Figure 10a (R1 and R2).

Our finding that R7 is not competitive with R6 in the butene system is also of value in deriving insight into the propene

dx.doi.org/10.1021/jp407986n | J. Phys. Chem. A 2013, 117, 13967−13975

reaction. The H-atom elimination pathway R7 for butene is analogous to R2 in the propene reaction, which is believed to be the sole source of 3-phenylpropene. In drawing conclusions from these analogies, it is important to remember that in the butene system, all products are formed from chemically indistinguishable reaction intermediates (Figure 10c) and are in direct competition with one another. In contrast, H-atom elimination in the propene system via R2 is only in direct competition with R1, and any competition between R2 and the other available channels (R3 and R4) requires isomerization between the 1- and 2-addition products. As noted above, the low barrier for isomerization and the RRKM calculations provide strong evidence that isomerization is much faster than product formation by bond fission under our experimental conditions.[16] Under such limiting conditions, all four decomposition pathways (R1−R4) can be considered to be in mutual competition, in a manner analogous to the competition (R5−R7) in the butene reaction. From the analogies between R7 and R2, as well as between R5 and R3, described above, we are thus tempted to suggest that in the propene system, the H-atom channels, R2 and R3, are not likely to be competitive with CH_3 elimination, R4. This would lead to the conclusion that in the propene system, the dominant source of H involves R1, which has no analogue in the *trans*-2-butene reaction, and that the dominant C_9H_{10} isomers are *cis*- and *trans*-1-phenylpropene. This conclusion is consistent with the earliest crossed beam studies using deuterated propenes, which reported an 85:15 branching ratio for 1-phenylpropene/3-phenylpropene.[15] However, more recent RRKM calculations have instead suggested the reverse behavior, with the 3-phenylpropene *dominating* the chemistry because of a slightly (∼1 kJ/mol) smaller barrier height for its production via C−H bond fission.[16,18]

In the newer CMB study at E_{coll} = 45 kJ/mol, the branching ratios for H or D atom elimination from the different propene carbon atom sites were not reported.[16] However, in the recent photoionization efficiency studies using tunable synchrotron radiation, it was found that the experimental data could be simulated by assuming dominant formation of 3-phenylpropene (I.E. = 8.40 eV), in apparent support of the newer electronic structure and RRKM calculations.[17] However, because of the similarity in the ionization energies for the different isomers,[17] other possible isomer branching ratios would also be consistent with the experimental measurements, including dominant formation of *trans*-1-phenylpropene (I.E. = 8.38 eV).[17]

While our observations appear to support the earlier CMB study in which 1- and 2-phenylpropene were identified as the primary C_9H_{10} isomers, with only minor formation of 3-phenylpropene,[15] the use of soft 9.9 eV photoionization detection of products from crossed-beam studies employing D isotope labeled propene would provide more definitive conclusions. We hope to carry out such studies in the future.

According to the previous calculations, phenyl radicals can abstract hydrogen atoms from propene forming C_6H_6 (benzene) + C_3H_5, with several different isomeric forms of C_3H_5 radical possible.[9,16,18] Abstraction of one of the three methyl H-atoms forming resonantly stabilized allyl radicals is most favorable energetically, with abstraction at the sp^2 hybridized carbon atoms leading to formation of 1- and 2-propenyl radicals.[9,18] To date, none of the CMB studies have addressed these channels. In principle, these channels can be most easily monitored by detecting C_6H_6 at its parent mass, m/e = 78. Unfortunately, because of the natural abundance of ^{13}C, background signals due to elastic and inelastic scattering of C_6H_5 is present, with intensities ∼6% of that at m/e = 77, making it impossible to detect nascent benzene from the abstraction channel at m/e = 78. However, using deuterated propene, abstraction of a D-atom produces C_6H_5D, which can be detected with high sensitivity at m/e = 79. Furthermore, by comparing the signals at m/e = 79 from reactions of 3,3,3-trideuteropropene to that from 1,1,2- trideuteropropene, it should be possible to assess the relative importance of abstraction at the methyl vs sp^2-hybridized carbon atoms in propene.

CONCLUSIONS

In the reaction of phenyl radicals with propene, both H-atom and CH_3 elimination products were observed at collision energies of 84 and 108 kJ/mol. At both collision energies, methyl radical elimination forming C_8H_8 was found to be dominant, with branching ratios for C_8H_8/C_9H_0 of 10 ± 1:1 and 3 ± 1:1 at 84 and 108 kJ/mol, respectively. The decrease in product branching ratio with increasing collision energy is consistent with RRKM predictions.[16] However, we find the methyl radical elimination channel to be considerably larger than inferred from the previous CMB studies[16] but comparable to those measured in a high-temperature pyrolysis reactor.[17]

Further insight into the reaction mechanism was gained by studying the reaction of phenyl radicals with *trans*-2-butene, where addition at each carbon atom leads to indistinguishable intermediates analogous to the 2-carbon addition intermediate in the propene reaction. In the reaction with *trans*-2-butene, elimination of CH_3 forming C_9H_{10} was observed with an upper limit of 3% for the H-atom elimination products. From analogies between the open reaction channels in the propene and *trans*-2-butene reactions, we suggest that in the reaction with propene that the minor H-atom elimination channel results from decomposition of the 1-carbon addition intermediate. While we tentatively suggest the reaction involves fission of the weakest C−H bond, producing *cis*- or *trans*-1-phenylpropene, definitive conclusions regarding the isomeric form of the C_9H_{10} product and the mechanisms for the abstraction reactions forming benzene await deuterium isotope labeling studies.

AUTHOR INFORMATION

Corresponding Author

*(H.F.D.) E-mail: hfd1@cornell.edu.

Notes

The authors declare no competing financial interest.

ACKNOWLEDGMENTS

This research was supported by the U.S. Department of Energy, under Grant DE-FG02-00ER15095 (free radical combustion chemistry). The development of the VUV light source was, in part, supported by the National Science Foundation under Grant CHE-0809622 (transition metal-hydrocarbon chemistry). We wish to acknowledge Ralf Kaiser, Alex Mebel, and David Collum for valuable discussions and suggestions regarding the phenyl + propene reaction dynamics.

REFERENCES

(1) Richter, H.; Howard, J. B. Formation of polycyclic aromatic hydrocarbons and their growth to soot-a review of chemical reaction pathways. *Prog. Energy Combust. Sci.* **2000**, *26*, 565−608.

(2) Miller, J. A.; Pilling, M. J.; Troe, J. Unraveling combustion mechanisms through a quantitative understanding of elementary reactions. *Proc. Combust. Inst.* **2005**, *30*, 43−88.
(3) Highwood, E. J.; Kinnersley, R. P. When smoke gets in our eyes: The multiple impacts of atmospheric black carbon on climate, air quality and health. *Environ. Int.* **2006**, *32*, 560−566.
(4) Shiraiwa, M.; Selzle, K.; Pöschl, U. Hazardous components and health effects of atmospheric aerosol particles: reactive oxygen species, soot, polycyclic aromatic compounds and allergenic proteins. *Free Radical Res.* **2012**, *46*, 927−939.
(5) Frenklach, M. Reaction mechanisms of soot formation in flames. *Phys. Chem. Chem. Phys.* **2002**, *4*, 2028−2037.
(6) Shukla, B.; Koshi, M. Comparative study on the growth mechanisms of PAHs. *Combust. Flame* **2011**, *158*, 369−375.
(7) Tokmakov, I. V.; Lin, M. C. Reaction of phenyl radicals with acetylene: Quantum chemical investigation of the mechanism and master equation analysis of the kinetics. *J. Am. Chem. Soc.* **2003**, *125*, 11397−11408.
(8) Tokmakov, I. V.; Lin, M. C. Combined quantum chemical/RRKM-ME computational study of the phenyl + ethylene, vinyl + benzene, and H + styrene reactions. *J. Phys. Chem. A* **2004**, *108*, 9697−9714.
(9) Park, J.; Nam, G. J.; Tokmakov, I. V.; Lin, M. C. Experimental and theoretical studies of the phenyl radical reaction with propene. *J. Phys. Chem. A* **2006**, *110*, 8729−8735.
(10) Casavecchia, P.; Leonori, F.; Balucani, N.; Petrucci, R.; Capozza, G.; Segoloni, E. Probing the dynamics of polyatomic multichannel elementary reactions by crossed molecular beam experiments with soft electron-ionization mass spectrometric detection. *Phys. Chem. Chem. Phys.* **2009**, *11*, 46−65.
(11) Balucani, N.; Leonori, F.; Casavecchia, P. Crossed molecular beam studies of bimolecular reactions of relevance in combustion. *Energy* **2012**, *43*, 47−54.
(12) Albert, D. R.; Davis, H. F. Studies of bimolecular reaction dynamicsusing pulsed high-intensity vacuum-ultraviolet lasers for photoionization detection. *Phys. Chem. Chem. Phys.* **2013**, *15*, 14566−14580.
(13) Hefter, H. J.; Hecht, T. A.; Hammond, G. S. Radical attack on propylene as studied by electron spin resonance. *J. Am. Chem. Soc.* **1972**, *94*, 2793−2797.
(14) Gu, X.; Kaiser, R. I. Reaction dynamics of phenyl radicals in extreme environments: A crossed molecular beam study. *Acc. Chem. Res.* **2009**, *42*, 290−302.
(15) Zhang, F.; Gu, X.; Guo, Y.; Kaiser, R. I. Reaction dynamics of phenyl radicals (C_6H_5) with propylene (C_3H_6) and its deuterated isotopologues. *J. Phys. Chem. A* **2008**, *112*, 3284−3290.
(16) Kaiser, R. I.; Parker, D. S. N.; Goswami, M.; Zhang, F.; Kislov, V. V.; Mebel, A. M.; Aguilera-Iparraguirre, J.; Green, W. H. Crossed beam reaction of phenyl and D5-phenyl radicals with propene and deuterated counterparts-competing atomic hydrogen and methyl loss pathways. *Phys. Chem. Chem. Phys.* **2012**, *14*, 720−729.
(17) Zhang, F.; Kaiser, R. I.; Golan, A.; Ahmed, M.; Hansen, N. A VUV photoionization study of the combustion-relevant reaction of the phenyl radical (C_6H_5) with propylene (C_3H_6) in a high temperature chemical reactor. *J. Phys. Chem. A* **2012**, *116*, 3541−3546.
(18) Kislov, V. V.; Mebel, A. M.; Aguilera-Iparraguirre, J.; Green, W. H. Reaction of phenyl radical with propylene as a possible source of indene and other polycyclic aromatic hydrocarbons: An ab initio/RRKM-ME study. *J. Phys. Chem. A* **2012**, *116*, 4176−4191.
(19) Taatjes, C. A.; Hansen, N.; McIlroy, A.; Miller, J. A.; Senosiain, J. P.; Klippenstein, S. J.; Qi, F.; Sheng, L.; Zhang, Y.; Cool, T. A.; Wang, J.; Westmoreland, P. R.; Law, M. E.; Kasper, T.; Kohse-Höinghaus, K. Enols are common intermediates in hydrocarbon oxidation. *Science* **2005**, *308*, 1887−1889.
(20) Welz, O.; Savee, J. D.; Osborn, D. L.; Vasu, S. S.; Percival, C. J.; Shallcross, D. E.; Taatjes, C. A. Direct kinetic measurements of criegee intermediate (CH_2OO) formed by reaction of CH_2I with O_2. *Science* **2012**, *335*, 204−207.
(21) Willis, P. A.; Stauffer, H. U.; Hinrichs, R. Z.; Davis, H. F. Rotatable source crossed molecular beams apparatus with pulsed ultraviolet/vacuum ultraviolet photoionization detection. *Rev. Sci. Instrum.* **1999**, *70*, 2606−2614.
(22) Proch, D.; Trickl, T. A high-intensity multi-purpose piezoelectric pulsed molecular beam source. *Rev. Sci. Instrum.* **1988**, *60*, 713−716.
(23) Proctor, D. L.; Albert, D. R.; Davis, H. F. Improved piezoelectric actuators for use in high-speed pulsed valves. *Rev. Sci. Instrum.* **2009**, *81*, 023106.
(24) Sveum, N. E.; Goncher, S. J.; Neumark, D. M. Determination of absolute photoionization cross sections of the phenyl radical. *Phys. Chem. Chem. Phys.* **2006**, *8*, 592−598.
(25) Albert, D. R.; Davis, H. F. Collision complex lifetimes in the reaction $C_6H_5 + O_2 \rightarrow C_6H_5O + O$. *J. Phys. Chem. Lett.* **2010**, *1*, 1107.
(26) Albert, D. R.; Proctor, D. L.; Davis, H. F. High-intensity coherent vacuum ultraviolet source using unfocussed commercial dye lasers. *Rev. Sci. Instrum.* **2013**, *84*, 063104.
(27) Smith, A. V.; Alford, W. J. Practical guide for 7S resonant frequency mixing in mercury: generation of light in the 230−185- and 140−120 nm ranges. *J. Opt. Soc. Am. B* **1987**, *4*, 1765−1770.
(28) Muller, C. H., III; Lowenthal, D. D.; DeFaccio, M. A.; Smith, A. V. High-efficiency, energy-scalable, coherent 130-nm source by four-wave mixing in Hg vapor. *Opt. Lett.* **1988**, *13*, 651−653.
(29) Schroden, J. J.; Teo, M.; Davis, H. F. Dynamics of CO elimination from reactions of yttrium atoms with formaldehyde, acetaldehyde, and acetone. *J. Chem. Phys.* **2002**, *117*, 9258−9265.
(30) Zhou, Z.; Xie, M.; Wang, Z.; Qi, F. Determination of absolute photoionization cross-sections of aromatics and aromatic derivatives. *Rapid Commun. Mass Spectrom.* **2009**, *23*, 3994−4002.
(31) Adam, T.; Zimmermann, R. Determination of single photon ionization cross sections for quantitative analysis of complex organic mixtures. *Anal. Bioanal. Chem.* **2007**, *389*, 1941−1951.
(32) Linstrom, P. J.; Mallard, W. G. *NIST Chemistry WebBook*; NIST: Gaithersburg, MD, 2005.
(33) Robinson, J. C.; Sveum, N. E.; Neumark, D. M. Determination of absolute photoionization cross sections for vinyl and propargyl radicals. *J. Chem. Phys.* **2003**, *119*, 5311−5314.
(34) Morton, M. L.; Butler, L. J.; Stephenson, T. A.; Qi, F. C−Cl bond fission, HCl elimination, and secondary radical decomposition in the 193 nm photodissociation of allyl chloride. *J. Chem. Phys.* **2002**, *116*, 2763−2775.
(35) Aguirre, F.; Pratt, S. T. Photoionization of vibrationally hot CH_3 and CF_3. *J. Chem. Phys.* **2005**, *122*, 234303.
(36) Fan, H.; Pratt, S. T. Near-threshold photoionization of hot isopropyl radicals. *J. Chem. Phys.* **2006**, *124*, 114312.
(37) Gross, R. L.; Liu, X.; Suits, A. G. The ultraviolet photodissociation of 2-chlorobutane: an imaging study comparing state-resolved and universal probe techniques. *Chem. Phys. Lett.* **2002**, *362*, 229−234.